

PAPER • OPEN ACCESS

Deformation and thinning field prediction for HFQ® formed panel components using convolutional neural networks

To cite this article: H R Attar *et al* 2021 *IOP Conf. Ser.: Mater. Sci. Eng.* **1157** 012079

View the [article online](#) for updates and enhancements.

Deformation and thinning field prediction for HFQ® formed panel components using convolutional neural networks

H R Attar*, H Zhou, and N Li

Dyson School of Design Engineering, Imperial College London, London SW7 2DB, UK

*corresponding author E-mail: h.attar19@imperial.ac.uk

Abstract. The novel Hot Forming and cold die Quenching (HFQ®) process can provide cost-effective and complex deep drawn solutions through high strength aluminium alloys. However, the unfamiliarity of the new process prevents its widescale adoption in industrial settings, while accurate Finite Element (FE) simulations using the most advanced material models take place late in design processes and require forming process expertise. Machine learning technologies have recently been proven successful in learning complex system behaviour from representative examples and have the potential to be used as design support tools for new forming technologies such as HFQ®. This study, for the first time, presents a novel application of a Convolutional Neural Network (CNN) based surrogate to predict the deformation and thinning fields for variable deep drawn geometries formed using HFQ® technology. A dataset based on deep drawn geometries and corresponding FE results is generated and used to train the model. The results show that near indistinguishable full field predictions in real time are obtained from the surrogate when compared with HFQ® simulations. This technique can be adopted in industrial settings to aid in both concept and detailed component design for complex-shaped panel components formed under HFQ® conditions, without underlying knowledge of the forming process.

1. Introduction

Nowadays, the transportation sector is recognized as a significant contributor to the ever-growing concerns surrounding global environmental impact. Recent figures by the Office for National Statistics reveal that transport is responsible for 28% of all greenhouse gas emissions in the United Kingdom [1]. Besides using alternatives to carbon-intensive power trains, vehicle lightweighting is one of the most effective strategies to reduce vehicle use-phase emissions [2].

Aluminium alloys are a family of lightweight metals beginning to find widespread application in the automotive industry. The exceptional strength to weight ratio makes the high strength aluminium alloys particularly attractive, with the potential to replace equivalent heavier steels traditionally used [2]. However, aluminium alloys exhibit poor formability under cold working conditions and display a significant degree of springback once the forming tools are removed [3]. To overcome these limitations, the novel Hot Forming and cold die Quenching (HFQ®) process has been developed by Lin *et al.* [4]. A summary of the HFQ® process is seen in Figure 1, and described further in [5].



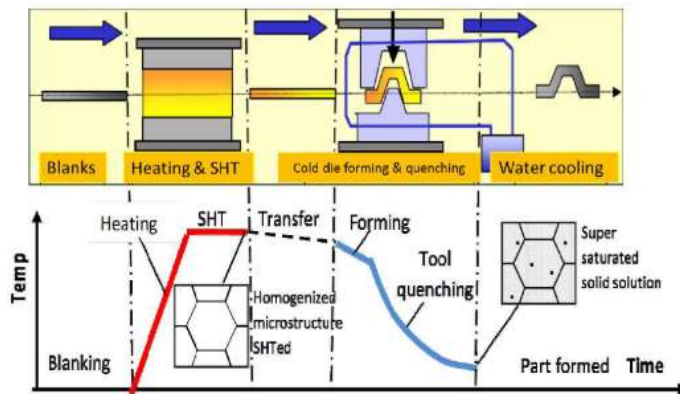


Figure 1. A summary of the HFQ® forming process: aluminium blanks are heated to their Solution Heat Treatment (SHT) temperature before being formed and quenched by cold tools, highlighting the non-isothermal nature of the process [6].

Due to the increased material formability at elevated temperatures, HFQ® enables complex deep drawn shapes with tight radii to be formed from high strength aluminium alloys [5]. However, during the industrial exploitation process, it has been observed that the uptake of HFQ® technology is limited by its lack of familiarity among industrial designers. Developments made in published literature focus on advanced material models [5,7–9] that predict the material constitutive behaviour and forming limits under HFQ® conditions. These models are then used to accurately simulate the forming response of HFQ® formed components using Finite Element (FE) simulations [10]. Though useful, forming simulations usually take place late in design processes [11] and require significant process expertise. Consequently, more familiar cold formed, or higher embedded CO₂ solutions may be used instead, meaning the potential weight saving and design capabilities of HFQ® are not fully realized. To realize its full potential, HFQ® technology should be adopted from the onset of a design process.

The advent of machine learning (ML) in recent times has introduced a means for the establishment of time efficient process models. Fundamentally, ML approaches can learn complex system dynamics from simulation data using a dataset comprising of input-target examples, known as training. Once training is complete, the models can be used for rapid prediction of system behaviour from unseen input data [12]. Such models are often referred to as surrogate models or metamodels in literature.

ML technologies based on FE simulation data have been widely used to support the design for manufacture of sheet forming processes. As typical examples, Ambrogio *et al.* [13] employed a Kringing surrogate model technique to establish a relationship between incremental sheet forming processing parameters and final sheet thickness. Harsch *et al.* [14] used surrogate models to construct forming window maps for a cold stamping process. Zimmerling *et al.* [15] went further and extended their model predictions to variable geometries. They established an easy to evaluate Gaussian Process regressor which can predict the maximum fabric shear angle in a composite forming process for geometries unseen during training. However, the above techniques are limited to scenarios where the inputs can be parameterized using relatively few parameters. Hundreds of forming simulations may be carried out by engineering companies every day which result in an accumulation of large engineering datasets, which may not share common CAD parameterizations, especially for complex geometries. Such data therefore cannot be exploited using parametric methods.

In addition to the above limitations, available FE simulation data is usually condensed to a single scalar such as maximum strain, resulting in information loss as mentioned by Zhou, Li & Xu [16]. Other references predict full FE field data from all elements in a FE mesh using deep neural networks (DNNs). For example, Liang *et al.* [17] established a DNN based model to predict the entire stress distribution in FE models of a human thoracic aorta and Pfrommer *et al.* [18] used DNNs to predict shear angles from over 24,000 elements in textile forming simulations. However, these models predict the element wise simulation results; the element type, numbering strategy and position must be

common between the training data and the model predictions. This mesh dependency impedes generalization in forming applications, since components are of different shapes and sizes.

Recently, researchers have turned to Convolutional Neural Networks (CNNs) in conjunction with image-based representations of boundary conditions and FE results, to detach from element wise dependencies when constructing surrogate models of FE simulations [19–25]. CNNs are a particular class of neural networks that have gained popularity when working with spatially structured data such as grids or images. Nie, Jiang & Kara [26] used CNNs to predict the stress fields in 2D cantilever structures deforming elastically. Thuerey *et al.* [27] predicted fluid flow solutions over varying airfoil shapes at different flow conditions. Cheng *et al.* [23] predicted spatial and temporal tsunami wave fluid solutions. These studies show that CNNs provide strong predictive capabilities when modelling highly non-linear physical systems, analogous to HFQ®. The complex non-isothermal nature of the HFQ® process together with the strain-rate dependency of aluminium alloys at elevated temperatures [5,7] make the process a challenging physical system to accurately model using surrogate techniques.

The purpose of this study is to present a novel application of a CNN based surrogate to predict the deformation and thinning fields in real time for variable deep drawn geometries formed using HFQ® technology. A comprehensive CNN based surrogate of the FE process is constructed, suitable for use by component designers during early design phases. This approach enables rapid prediction of full field forming responses for complex HFQ® formed geometries without specific CAD parametric schemes, FE mesh dependencies or underlying knowledge of the forming process. It is to be noted that this technique can also be applied to simpler and more familiar cold forming processes. Consequently, this paper provides an invaluable design support tool, enabling designers to become familiar with how thinning fields change under HFQ® conditions due to variations in component geometric features, and compare solutions obtained from different forming technologies in real time.


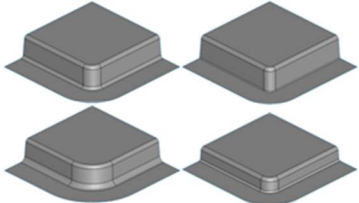


2. Data acquisition

Prior to training the CNN based model, data in the form of geometries and corresponding simulation HFQ® simulation results is required. Details concerning the dataset used in this study and data preparation for network training are discussed in this section.

2.1. Geometry definition and design of experiments

Deep drawn box geometries were considered in this study, which are widely adopted but challenging geometries to form. More specifically, flanged shrink corners are investigated, which are formed when blank material is drawn into a plan view radius that is smaller than the blank corner radius, as described by Horton *et al.* [11]. Due to their symmetry, quarter boxes were modelled, with a half side length of 500mm. Table 1 shows details of the parameterisation scheme employed to generate CAD geometries.

Table 1. Geometric parameters, bounds and example geometries

Geometric Parameters	Symbol	Description	Bounds	Example Geometries
	r_{die}	Die radius	5 -30 mm	
	r_{punch}	Punch radius	5-30 mm	
	r_{plan}	Plan view radius	40-120 mm	
	H	Design height	50-150 mm	

As a first study, a database consisting of 1800 geometries was built. To ensure good distribution of geometries within the design space, the Latin hypercube design of experiments (DoE) technique was employed. The generation of the tool and blank CAD variants was automated using the VBA programming language in SolidWorks. Upper and lower bounds for each geometric parameter, shown in Table 1, were assigned during the automation scheme. Further, filtering rules were applied to preserve geometric integrity during the automation process as described by Ramnath *et al.* [28,29].

2.2. HFQ® forming simulations

FE models were built based on the generated CAD models and the FE solver PAM-STAMP was used to simulate the non-isothermal deep drawing processes. To capture the material constitutive behaviour under HFQ® conditions, the FE simulations used viscoplastic material data for AA6082 under various temperatures and strain rates, adapted from El Fakir [30], shown in Figure 2. The initial blank temperature was set to 500°C for AA6082 [5], while the tools were set to 25°C. Simulation setup parameters, such as friction and heat transfer coefficients were assumed identical to those used in [30].

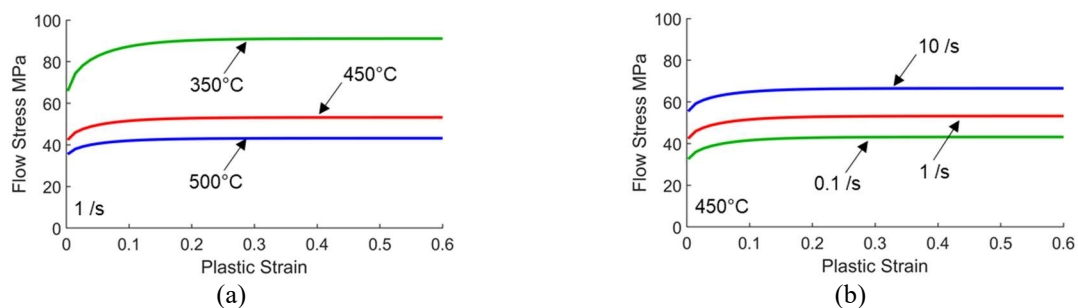


Figure 2. Temperature and rate dependant stress-strain material data for AA6082 used in HFQ® simulations.

2.3. CNN training data pre-processing

An undercut free geometry is a necessary requirement to avoid collision with forming tools. Both the 3D die geometry and 2D blank can therefore be projected onto a 2D planes without spatial information loss. The 2D plane used was a cartesian grid (i.e. image) of a fine 512*512 pixel resolution to capture small geometric features on the tool, such as sharp tool radii. Geometry height and thickness contours were used as the out of plane dimension for the die and blank images respectively. An example is shown in Figure 3. These images served as the input data for the CNN training and evaluation.

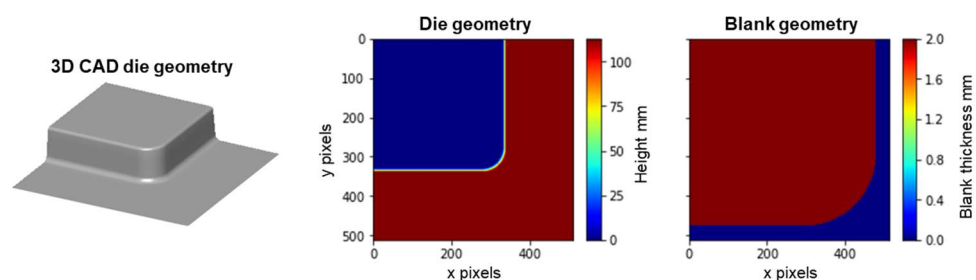


Figure 3. Image representation of input data for CNN training and evaluation: 3D die geometries and blanks are projected onto a 2D images.

The target data was prepared in a similar manner. Nodal displacement fields in x y and z directions, together with thinning fields at the final forming step were extracted from all the deep drawing simulations. This data was then plotted on the 2D undeformed blank and projected onto 2D cartesian grids of resolution 256*256, which resulted in image representations of the simulation results. A representative example is shown in Figure 4, corresponding to the input data seen in Figure 3.

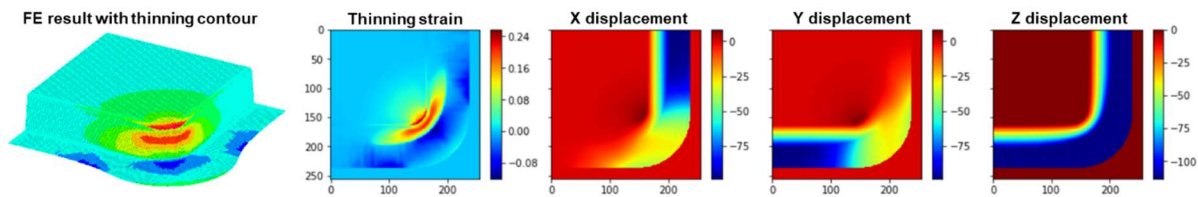


Figure 4. Image representation of target data for CNN training and evaluation: FE simulation results plotted on the undeformed blank and projected onto 2D images. Displacement colour scale in mm, image x-y axis in pixels.

3. Neural network architecture and training

A Res-SE-U-Net architecture was employed as the CNN based surrogate model in this study, shown in Figure 5. Res-SE-U-Nets have recently been proven to display exceptional performance in image-to-image mapping tasks in several studies [16,21,22]. This architecture consists of a down sampling encoder comprising of convolutional layers, bottleneck with Res-SE layers and an up-sampling decoder comprising of up convolutional layers. Details on Res-SE layers can be found in [31,32]. The encoder-decoder structure with the skip connections which copy and concatenate intermediate feature maps are typical features of U-net architectures, introduced in [33]. Batch normalisation (BN) layers followed by a ReLU activation layer were used after all convolution operations in the encoder and decoder. Kernel size, stride and padding for all convolutional operations were selected such that feature maps with powers of 2 spatial dimensions were established throughout the network.

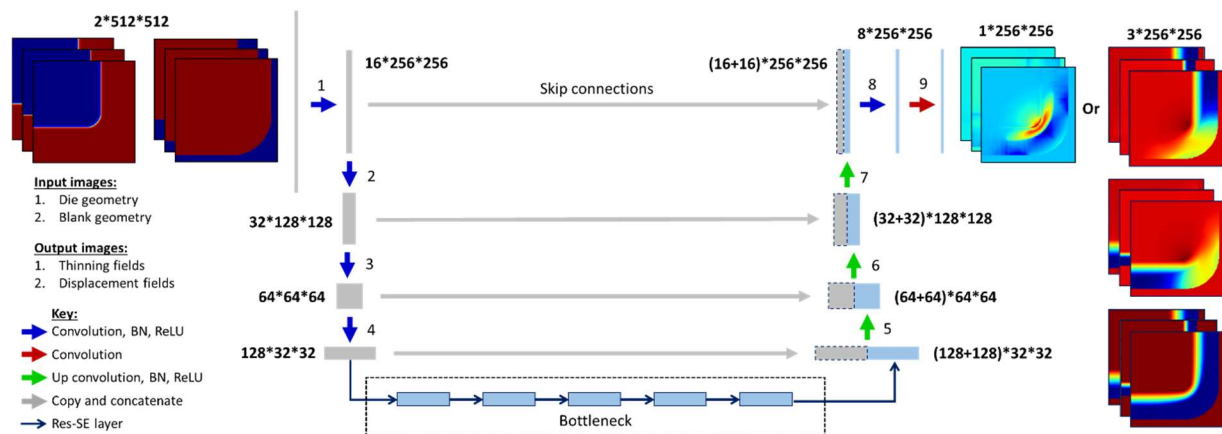


Figure 5. Res-SE-U-Net architecture of the neural network: a U-Net structure with Res-SE architectural blocks at its bottleneck.

The dataset contained 1800 unique instances of die and blank geometry images as inputs, and corresponding FE simulation results images as targets, and followed a random 90% training and 10% testing data split. Each input image was of size $2 \times 512 \times 512$, with the 2 representing a die geometry channel and a blank shape channel. As for the target images, the thinning images were of size $1 \times 256 \times 256$ and the displacement images were of size $3 \times 256 \times 256$, with the 3 representing x y and z displacements. Separate Res-SE-U-Nets were trained on input-thinning and input-displacement data pairs to prevent the sharing of network weights which would otherwise occur if both types of outputs were to be predicted simultaneously by a single network. These networks both followed an identical architecture to Figure 5 but varied only in the output channel size, as seen in the figure.

The models were trained using the commonly recommended Adam optimiser with default parameters using the PyTorch framework. Through an iterative training process, the optimiser sought to find the combination of network parameters such that the mean square error between the ground

truth (i.e. real target) images and network predictions was minimised. In this way, the network was able to learn a function that can predict the HFQ® simulation results given a new corner geometry.

4. Network performance evaluation

After the networks finished training, their performance was evaluated by comparing the network predictions with ground truths based on HFQ® FE simulations. Figure 6 compares ground truth thinning distributions with those predicted by the network from five randomly sampled cases from the test dataset. These distributions were obtained by presenting images of new geometries to the network, as inputs, which were unseen during training. A good agreement between ground truths and network predictions can be seen.

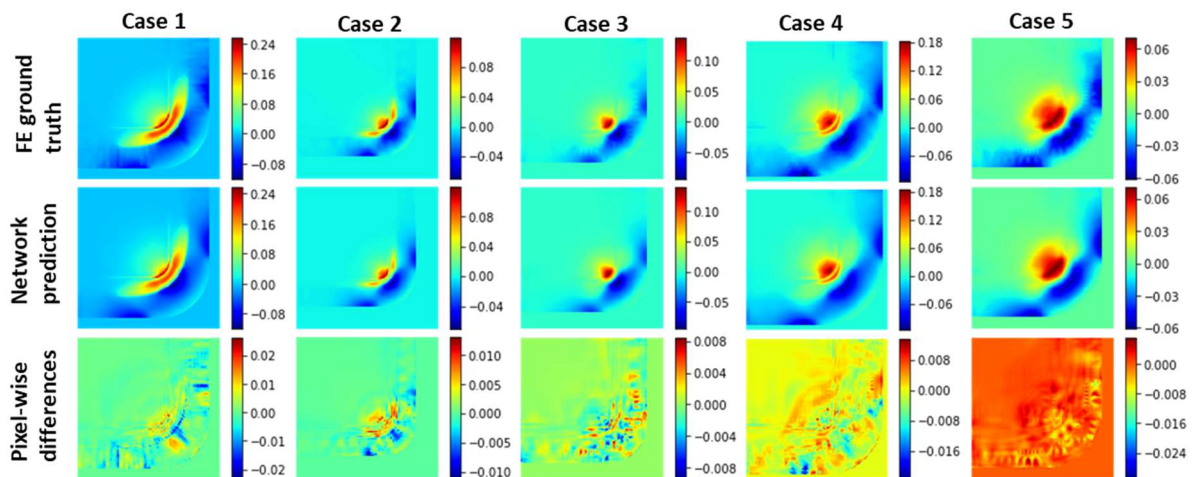


Figure 6. Comparison of thinning distributions between ground truths and network predictions, and their pixel wise differences, for five random test set cases. Contours plotted on undeformed blank geometry.

Similar comparison between the 2D x , y , and z displacement fields were also made where equally good predictions were seen and are presented in the Appendix. By applying the 2D displacement vector fields to uniform cartesian grids, 3D representations of the as-formed components were generated. The thinning fields were then be superimposed, and a comparison between the network predictions and ground truths for Case 1 and Case 5 from Figure 6 can be seen in Figure 7.

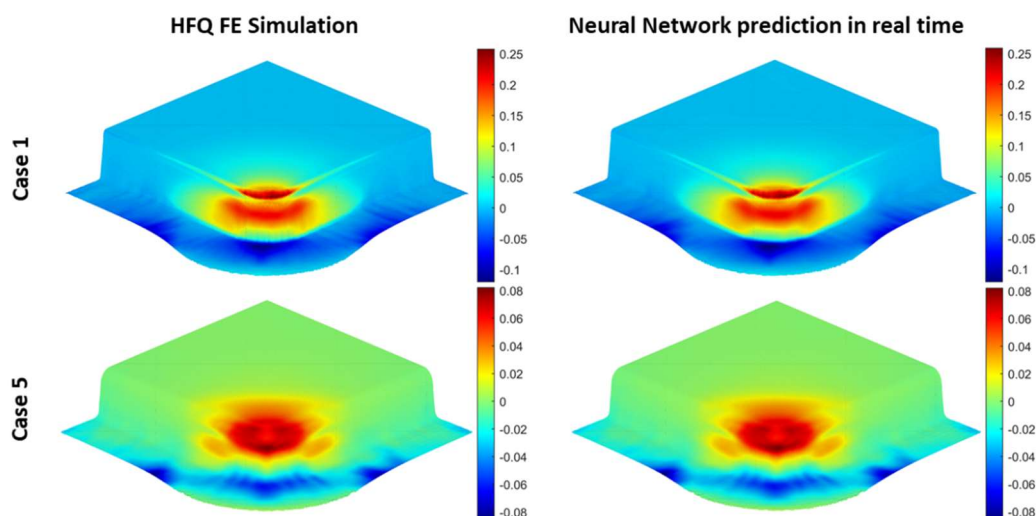


Figure 7. 3D as-formed components with thinning distributions from HFQ® FE simulations and ones predicted by the networks in real time for Case 1 and Case 5 in Figure 6.

5. Robustness to corrupt samples in the training set

Residual errors of maximum thinning values and mean thinning values from the thinning distributions between ground truths and network predictions for all samples were calculated and plotted in Figure 8. The majority of samples lie close to zero error when evaluating both max values and distribution mean values, suggesting near indistinguishable distributions, as seen in Figure 7. However, a small number of samples show large outlier error peaks. These samples were further investigated.

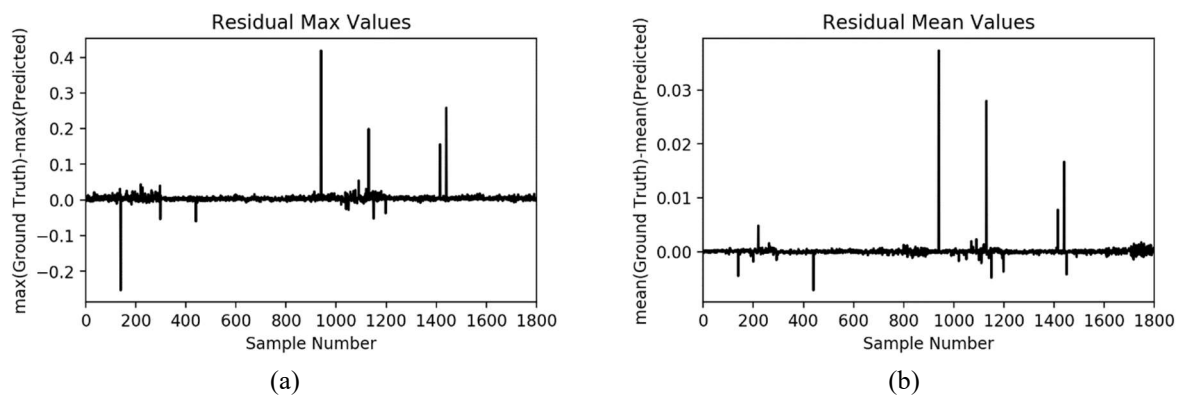


Figure 8. Spectrums of thinning distribution residuals (a) maximum values and (b) mean values between ground truths and network predictions for samples in the complete dataset.

Inspecting the data responsible for the error peaks revealed that these errors were due to corrupt samples present in the training data. The FE models responsible for these samples used improper mesh sizes. The slave surface (blank) element size was larger than the master surface (tools) element size, resulting in numerical errors when resolving the contact conditions during the FE computation, leading to mesh distortions. The FE computations for the corrupt samples were redone using a finer blank mesh size which led to reasonable results. A representative example is shown in Figure 9. Remarkably, the original network prediction matched the corrected FE simulation result, even though it was presented with the corrupt samples during training. For practical applications, it is imperative to ensure an outlier-free dataset is used, however this exercise suggests that the network did indeed learn the underlying distributions from the HFQ® data and was therefore robust to spurious outliers.

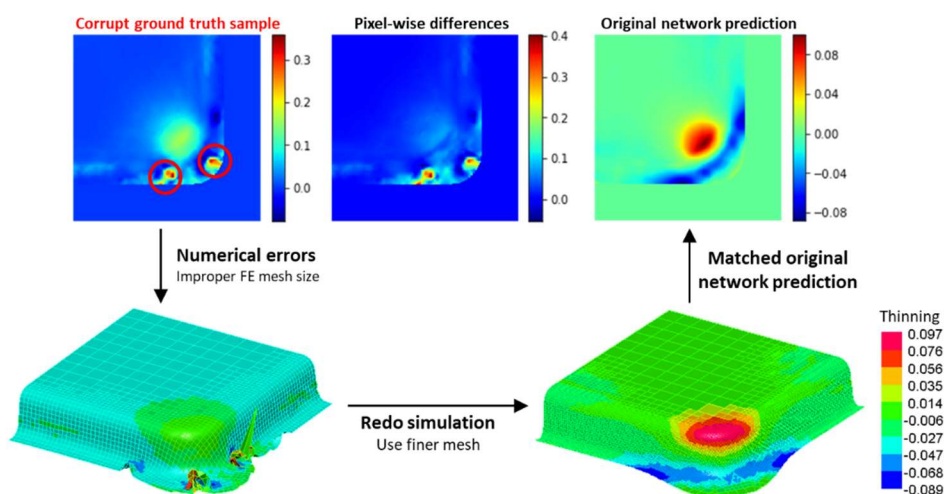


Figure 9. Large pixel-wise differences between ground truth sample and original network prediction due to numerical errors in the ground truth sample. Network was able to evade the corrupt sample during training and produced a sound prediction.

6. Conclusions

HFQ® is a new hot stamping technology that can provide a means of deep drawing complex panel components from high strength aluminium alloys. However, the uptake of HFQ® is limited by its unfamiliarity among industrial designers. In response, this paper presents a novel design support tool for HFQ® applications. A CNN based surrogate was employed which proved capable of learning the underlying distributions from HFQ® forming simulation data. Post form thinning and displacement distributions were predicted by the networks which not only allowed for a 3D as-formed representation in real time but were near indistinguishable from the FE simulation counterparts. The network can therefore provide a fast component feasibility assessment during early stage design without demanding intricate underlying knowledge of the HFQ® process from component designers.

Acknowledgments

The authors thank the funding support by Impression Technologies Ltd, UK Engineering and Physical Sciences Research Council, Shougang Research Institute of Technology, and the Chinese Scholarship Council. Software and technical support from Rajab Said and Mustapha Ziane from ESI Group, and technical support from Alistair Foster from Impression Technologies Ltd are also gratefully acknowledged. HFQ® is a registered trademark of Impression Technologies Ltd.

Appendix

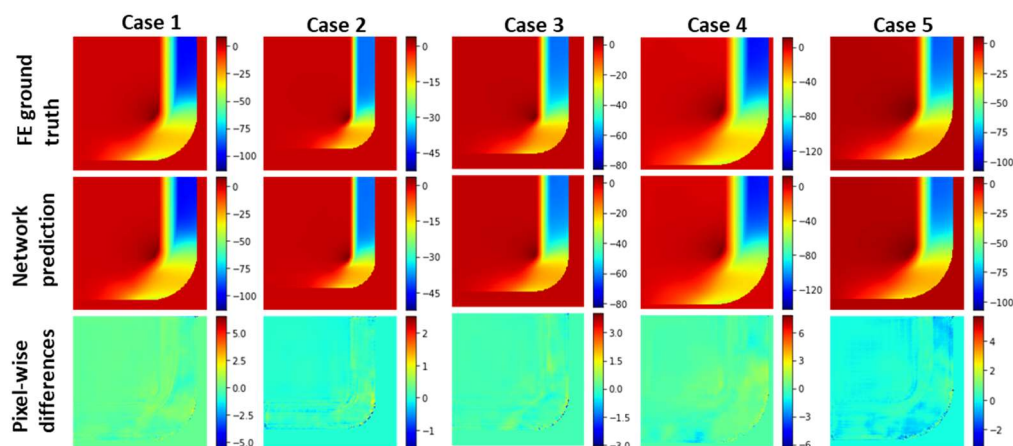


Figure A1. Comparison of x displacement distributions in mm with between ground truth network prediction, and pixel wise differences for five random test set cases. Contours plotted on undeformed blank geometry.

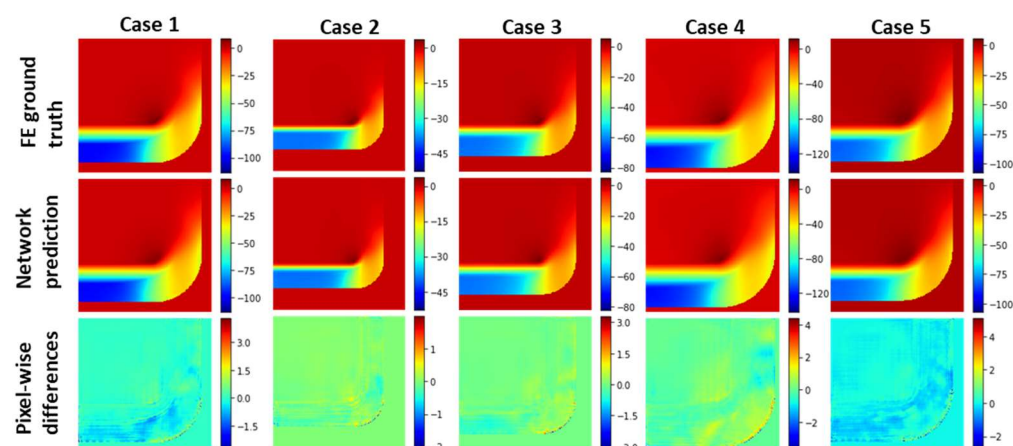


Figure A2. Comparison of y displacement distributions in mm with between ground truth network prediction, and pixel wise differences for five random test set cases. Contours plotted on undeformed blank geometry.

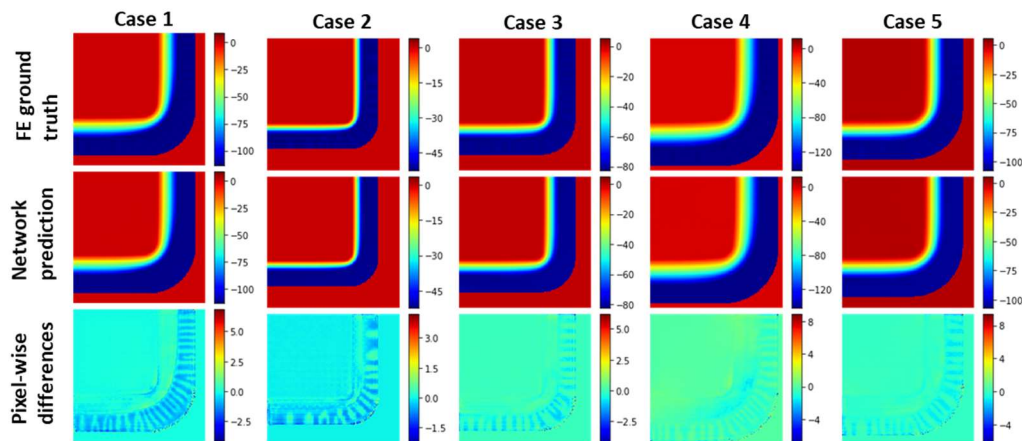


Figure A3. Comparison of z displacement distributions in mm with between ground truth network prediction, and pixel wise differences for five random test set cases. Contours plotted on undeformed blank geometry.

References

- [1] UK gov 2020 *2018 UK Greenhouse Gas Emissions, Final figures*
- [2] Rauegi M, El O, Wang L, Lin J and Morrey D 2014 Life cycle assessment of the potential environmental benefits of a novel hot forming process in automotive manufacturing *J. Clean. Prod.* **83** 80–6
- [3] Wang A, Zhong K, El Fakir O, Liu J, Sun C, Wang L L, Lin J and Dean T A 2017 Springback analysis of AA5754 after hot stamping: experiments and FE modelling *Int. J. Adv. Manuf. Technol.* **89** 1339–52
- [4] Lin J, Dean, Trevor A, Garrett, Richard P and Foster, Alistair D 2008 Process for forming aluminium alloy sheet component
- [5] Mohamed M S, Foster A D, Lin J, Balint D S and Dean T A 2012 Investigation of deformation and failure features in hot stamping of AA6082: Experimentation and modelling *Int. J. Mach. Tools Manuf.* **53** 27–38
- [6] Politis D J, Li N, Wang L, Lin J, Foster A D and Szegda D 2016 Prediction of Thinning Behavior for Complex-Shaped, Lightweight Alloy Panels Formed Through a Hot Stamping Process 395–401
- [7] Shao Z, Li N, Lin J and Dean T 2017 Formability evaluation for sheet metals under hot stamping conditions by a novel biaxial testing system and a new materials model *Int. J. Mech. Sci.* **120** 149–58
- [8] Lin J, Mohamed M, Balint D and Dean T A 2014 The development of continuum damage mechanics-based theories for predicting forming limit diagrams for hot stamping applications *Int. J. Damage Mech.* **23** 684–701
- [9] Wang A, Zheng Y, Liu J, El Fakir O, Masen M and Wang L 2016 Knowledge based cloud FE simulation a multi-objective FEA system for advanced FE simulation of hot stamping process *The 10th International Conference and Workshop on Numerical Simulation of 3D Sheet Metal Forming Processes*
- [10] El Fakir O, Wang L, Balint D, Dear J P, Lin J and Dean T A 2014 Numerical study of the solution heat treatment, forming, and in-die quenching (HFQ) process on AA5754 *Int. J. Mach. Tools Manuf.* **87** 39–48
- [11] Horton P M, Allwood J M, Cleaver C and Nagy-Sochacki A 2020 An experimental analysis of the relationship between the corner, die and punch radii in forming isolated flanged shrink corners from Al 5251 *J. Mater. Process. Technol.* **278**
- [12] Zimmerling C, Trippe D, Fengler B and Kärger L 2019 An approach for rapid prediction of textile draping results for variable composite component geometries using deep neural

- networks *AIP Conf. Proc.* **2113**
- [13] Ambrogio G, Ciancio C, Filice L and Gagliardi F 2017 Innovative metamodelling-based process design for manufacturing: an application to Incremental Sheet Forming *Int. J. Mater. Form.* **10** 279–86
- [14] Harsch D, Heingärtner J, Hortig D and Hora P 2016 Process windows for sheet metal parts based on metamodels *J. Phys. Conf. Ser.* **734**
- [15] Zimmerling C, Dörr D, Henning F and Kärger L 2018 A meta-model based approach for rapid formability estimation of continuous fibre reinforced components *AIP Conf. Proc.* **1960**
- [16] Zhou H, Li N and Xu Q 2020 A study on using image based machine learning methods to develop the surrogate models of stamp forming simulations *arXiv*
- [17] Liang L, Liu M, Martin C and Sun W 2018 A machine learning approach as a surrogate of finite element analysis-based inverse method to estimate the zero-pressure geometry of human thoracic aorta *Int. j. numer. method. biomed. eng.* **34** 1–11
- [18] Pfrommer J, Zimmerling C, Liu J, Kärger L, Henning F and Beyerer J 2018 Optimisation of manufacturing process parameters using deep neural networks as surrogate models *Procedia CIRP* **72** 426–31
- [19] Obiols-Sales O, Vishnu A, Malaya N and Chandramowliswharan A 2020 CFDNet: A deep learning-based accelerator for fluid simulations *Proc. Int. Conf. Supercomput.*
- [20] Donglin C, Gao X, Xu C, Chen S, Fang J, Wang Z and Wang Z 2020 *FlowGAN: A Conditional Generative Adversarial Network for Flow Prediction in Various Conditions*
- [21] Nie Z, Lin T, Jiang H and Kara L B 2020 TopologyGAN: Topology Optimization Using Generative Adversarial Networks Based on Physical Fields Over the Initial Domain *Preprint*
- [22] Jiang H, Nie Z, Yeo R, Farimani A B and Kara L B 2020 *StressGAN: A Generative Deep Learning Model for 2D Stress Distribution Prediction*
- [23] Cheng M, Fang F, Pain C C and Navon I M 2020 Data-driven modelling of nonlinear spatio-temporal fluid flows using a deep convolutional generative adversarial network *Comput. Methods Appl. Mech. Eng.* **365** 113000
- [24] Guo X, Li W and Iorio F 2016 Convolutional neural networks for steady flow approximation *Proc. ACM SIGKDD Int. Conf. Knowl. Discov. Data Min.* **13-17-Aug** 481–90
- [25] Wu H, Liu X, An W, Chen S and Lyu H 2020 A deep learning approach for efficiently and accurately evaluating the flow field of supercritical airfoils *Comput. Fluids* **198** 104393
- [26] Nie Z, Jiang H and Kara L B 2020 Stress Field Prediction in Cantilevered Structures Using Convolutional Neural Networks *J. Comput. Inf. Sci. Eng.* **20** 1–8
- [27] Thuerey N, Weißenow K, Prantl L and Hu X 2020 Deep Learning Methods for Reynolds-Averaged Navier–Stokes Simulations of Airfoil Flows *AIAA J.* **58** 25–36
- [28] Ramnath S, Haghghi P, Ma J, Shah J J and Detwiler D 2020 Design science meets data science: Curating large design datasets for engineered artifacts *Proceedings of the ASME 2020* pp 1–14
- [29] Ramnath S, Haghghi P, Kim J H, Detwiler D, Berry M, Shah J J, Aulig N, Wollstadt P and Menzel S 2019 Automatically generating 60,000 CAD variants for big data applications *Proc. ASME Des. Eng. Tech. Conf.* **1** 1–12
- [30] El Fakir O 2015 *Studies on the Solution Heat Treatment, Forming and in-Die Quenching Process in the Production of Lightweight Alloy Components* (Imperial College London) PhD Thesis
- [31] Hu J, Shen L and Sun G 2018 Squeeze-and-Excitation Networks *Cypr* 7132–41
- [32] He K, Zhang X, Ren S and Sun J 2016 Deep residual learning for image recognition *Proc. IEEE Comput. Soc. Conf. Comput. Vis. Pattern Recognit.* 770–8
- [33] Ronneberger O, Fischer P and Brox T 2015 U-net: Convolutional networks for biomedical image segmentation *Medical Image Computing and Computer-Assisted Intervention – MICCAI 2015* vol 9351 pp 234–41